Dendritic Cells from the Human Female Reproductive Tract Rapidly Capture and respond to HIV

M Rodriguez-Garcia, MD, PhD[1],*, **Zheng Shen, MD[1]**, **Fiona D. Barr[1]**, **Austin W. Boesch[2]**, **Margaret E. Ackerman, PhD[2]**, **John C. Kappes, PhD[3,4]**, **Christina Ochsenbauer, PhD[3]**, and **Charles R. Wira, PhD[1]**

[1]Department of Physiology and Neurobiology, Geisel School of Medicine at Dartmouth, Lebanon, NH, USA

[2]Thayer School of Engineering, Dartmouth College, Hanover, NH

[3]Department of Medicine and UAB Center for AIDS Research, University of Alabama at Birmingham, AL

[4]Birmingham Veterans Affairs Medical Center, Research Service Birmingham, AL

Abstract

Dendritic cells (DCs) throughout the female reproductive tract (FRT) were examined for phenotype, HIV capture ability and innate anti-HIV responses. Two main CD11c+ DC subsets were identified: CD11b+ and CD11b^low DCs. CD11b+CD14+ DCs were the most abundant throughout the tract.A majority of CD11c+CD14+ cells corresponded to CD1c+ myeloid DCs while the rest lacked CD1c and CD163 expression (macrophage marker) and may represent monocyte-derived cells. Additionally we identified CD103+ DCs, located exclusively in the endometrium, while DC-SIGN+ DCs were broadly distributed throughout the FRT. Following exposure to GFP-labeled HIV particles, CD14+ DC-SIGN+ as well as CD14+ DC-SIGN- cells captured virus, with approximately 30% of these cells representing CD1c+ myeloid DCs. CD103+ DCs lacked HIV capture ability. Exposure of FRT DCs to HIV induced secretion of CCL2, CCR5 ligands, IL-8, elafin and SLPI within 3h of exposure, while classical pro-inflammatory molecules did not change and IFNα2 and IL10 were undetectable. Furthermore, elafin and SLPI up-regulation, but not CCL5, were suppressed by estradiol pretreatment. Our results suggest that specific DC subsets in the FRT have the potential for capture and dissemination of HIV, exert antiviral responses and likely contribute to the recruitment of HIV-target cells through the secretion of innate immune molecules.

*Corresponding author. Address correspondence to Dr. Marta Rodriguez-Garcia, Department of Physiology and Neurobiology, Geisel School of Medicine at Dartmouth, One Medical Center Drive, Lebanon, NH 03756. Fax number: 603-6507717. Telephone number: 603-6502583. Marta.Rodriguez.Garcia@dartmouth.edu.

Introduction

Sexual transmission of HIV is the main route for HIV-acquisition in women worldwide[1]. HIV present in semen overcomes the epithelial barrier[2] to reach immune target cells in the female reproductive tract (FRT). As semen moves from the lower to the upper tract, HIV can interact with immune cells at different anatomical locations in the FRT. Because of their location within or beneath the epithelial lining, dendritic cells (DCs) are one of the first immune cells to encounter virus[3]. DCs have the ability to capture and transport virus to lymph nodes, where HIV trans-infection to T cells and infection dissemination is postulated to occur[4]. Alternatively, complete inactivation of HIV following viral contact with DCs could result in the induction of protective immune responses. Although this model has been proposed in vitro, little to nothing is known about resident DCs in the upper and lower FRT, the extent to which different subsets exist, and their roles in HIV acquisition.

Each anatomical region of the FRT displays distinct histological, immunological and functional characteristics[5]. The lower FRT (ectocervix and vagina), lined by stratified squamous epithelial cells, is colonized by commensal microbes and is the site for reception and accumulation of semen. In contrast, the upper FRT (uterine endocervix and endometrium) is lined by a single layer of columnar epithelium, has low levels of commensals and has adapted to support implantation and pregnancy[5]. As an example of immune compartmentalization, we recently demonstrated fundamental differences in Th17 $CD4^+$ T cell distribution and susceptibility to HIV infection in the FRT[6]. Th17 $CD4^+$ T cells, critical components of mucosal surfaces colonized by commensals[7], were more abundant in endocervix and ectocervix compared to the endometrium of premenopausal women. In addition, we found that $CD4^+$ T cells from ectocervix were the most susceptible to HIV infection in vitro, whereas HIV infection in $CD4^+$ T cells from the endometrium was barely detectable[6]. DCs are also particularly abundant at mucosal surfaces in contact with microbes, such as the lung, the gut and the genital tract. However, in the case of the FRT, DCs not only specialize to recognize potential invading pathogens but also to tolerate foreign antigens present in sperm and the developing fetus to allow reproduction[8]. Whether FRT immune compartmentalization extends to differences in DC populations is currently unknown. However, taking into consideration the differences in histology, function, microbiome and hormonal regulation at different locations in the FRT, we hypothesized that DCs may play different roles and display distinct phenotypes.

Unique to the immune system in the FRT is cyclical hormonal regulation that balances protection against infection and tolerance to allogeneic sperm and fetus[5]. Several studies demonstrate that menstrual status alters susceptibility to HIV and other STDs[5,9-11] and in vitro treatment of immune cells with hormones modulates their immune responses and susceptibility to HIV infection[12-15]. While monocyte-derived DC innate immune responses

are known to be sensitive to sex hormone regulation[16,17], potential hormonal effects on mucosal DC innate responses in the FRT are unknown.

Despite the critical role of DCs in sexual transmission of HIV and their potential for induction of protective immune responses, very little is known about DC subsets in the FRT and their responses to HIV infection. Most of our knowledge about mucosal DCs is extrapolated from mouse models or from human intestinal or skin DCs, models that are very different from the human FRT regarding function, commensal colonization and hormonal regulation. A few studies have analyzed DCs in the vagina and ectocervix[18-20] or in decidual tissue as they contribute to pregnancy[8], but potential differences between DCs at different FRT sites in non-pregnant women and their roles in anti-viral immune protection are unknown.

The goals of this study were first to characterize mucosal dendritic cell subsets relevant for HIV-acquisition at different anatomical regions in the FRT, and second to define the extent to which DCs exert early innate anti-viral responses after HIV exposure and their potential regulation by sex hormones. Data from this study should provide valuable information about the functional contributions of DCs to sexual HIV-acquisition.

Results

Two subsets of DCs (CD11c$^+$) are present in the FRT based on CD11b expression

Mononuclear phagocytes at mucosal surfaces represent a heterogeneous population that includes different types of DCs and macrophages[21]. To characterize tissue resident DCs in the FRT, as detailed in Methods, mixed cell suspensions from digested EM, CX and ECX were analyzed by flow cytometry (see gating strategy on Supplementary Figure 1). Phenotypic analysis allowed identification of three distinct populations based on CD11c and CD11b expression (Figure 1a): CD11c$^+$CD11b$^+$(red), CD11c$^+$CD11b^{low} (yellow) and CD11c^{low}CD11b$^+$ (blue). Each of these three populations displayed differential expression of CD14 and HLA-DR: CD11c$^+$CD11b$^+$ cells expressed the highest levels of both CD14 and HLA-DR (Figure 1b; red); CD11c$^+$CD11b^{low} cells (yellow) expressed low levels of CD14 and medium levels of HLA-DR; and CD11c^{low}CD11b$^+$ cells (blue) expressed medium levels of CD14 and low HLA-DR, likely representing mucosal macrophages. For our studies, we focused on mucosal DCs, defined as CD45$^+$, CD11c^{high} and HLA-DR$^+$ cells[22] (Figure 1a, red and yellow populations). Within CD11c$^+$ cells, CD11b$^+$ DCs were significantly more abundant than CD11b^{low} DCs in CX and ECX (Figure 1c; P=0.01 and P=0.0002 respectively). As shown in Figure 1d, within each tissue, CD11b$^+$ DCs expressed significantly higher levels of CD14 than CD11b^{low} DCs (P<0.0001, P<0.01 and P<0.0001 for EM, CX and ECX respectively). More than 80% of CD11b$^+$ DCs corresponded to CD14$^+$ DCs, while for the CD11b^{low} DC subset, CD14$^+$ DCs represented about 21%, 38% and 30% in EM, CX and ECX respectively. CD11b$^+$ DCs also expressed higher levels of HLA-DR (Figure 1e), although the difference with CD11b^{low} DCs was only significant in the EM (P<0.01). Interestingly, phenotypical differences between tissues were found exclusively for CD11b^{low} DCs, which selectively showed reduced expression of CD14 (Figure 1d; P<0.05) and HLA-DR^{high} (Figure 1E; P<0.05) in the EM compared to CX and ECX respectively. There was a trend for CD11b^{low} DCs to be more abundant in EM than CX

and ECX, but this difference was not significant (Figure 1c). Overall, these studies demonstrate that the dominant population of DCs within the EM, CX and ECX are CD11b⁺CD14⁺ DCs.

DC-SIGN and CD103 are differentially expressed on DCs from endometrium, endocervix and ectocervix

To compare for potential regional differences relevant for HIV acquisition, DC-SIGN and CD103 expression were evaluated on DCs from EM, CX and ECX. DC-SIGN (CD209), is a mannose receptor that mediates HIV capture and transmission from DCs to CD4⁺ T cells[4]. As seen in Figure 2a, DC-SIGN expression was detected on CD11b⁺ and CD11b^low DCs, with no significant differences between subsets. Interestingly, DC-SIGN⁺ DCs were more abundant in the endocervix compared to the EM (Figure 2a; p<0.05 for CD11b⁺ DCs and p<0.01 for CD11b^low DCs) and the ECX (p<0.05).

CD103 is an integrin that binds to E-Cadherin on epithelial cells and has been described to be involved in antigen sampling and migration to lymphoid tissue in the mouse and human intestine[22,23]. As shown in Figure 2b, CD103 was expressed on CD14⁻ DCs. CD103⁺ DCs were found almost exclusively in the EM, where they represented about 10% of CD11c⁺ cells (Figure 2c; left graph), compared to 2.5% and 1% of the DCs in CX (P<0.05) and ECX (P<0.0009) respectively. The differential expression of CD103 between anatomical locations was specific for DCs, since CD103 expression on T cells from the same donors was not different among sites (Figure 2c; right graph). Importantly, CD103⁺ DCs did not express DC-SIGN (Figure 2d), demonstrating that these are distinct cell subsets.

CD1c is highly expressed on DCs from the FRT

To better characterize FRT DCs and to differentiate between myeloid DCs and Langerhans cells, expression of CD1c and CD207 was determined.

CD1c⁺ was strongly expressed on DCs from EM, CX and ECX with more than 50% of positive cells and no differences between CD11b⁺ and CD11b^low DCs (Figure 3b; median of 68 and 57% respectively). A subset of CD1c+ DCs co-expressed CD14 (Figure 3c). As shown in Figure 3d, between 20 and 60% of cells co-expressed CD1c and CD14 within the CD11b⁺ population, while co-expression was only 25% or less on CD11b^low DCs (p<0.001), for which the majority of cells were CD1c⁺CD14⁻ (p<0.0001).

CD207 (Langerin) was found only on CD1c⁺ DCs (Figure 3a). CD207 expression was low but detectable on both CD11b⁺ and CD11b^low DCs. The highest expression was observed in the EM, with up to 15% of CD207⁺ cells. However, co-expression of CD1c and CD207 suggests that these cells are of interstitial origin and not Langerhans cells[24]. Neither CD207⁺ nor CD1c⁺ DCs co-expressed CD103, suggesting that they represent distinct DC subsets (Figure 3e).

Recognizing that tissue macrophages can express CD11c, CD11b, CD14 and HLA-DR, and that approximately 20-40% of cells within the CD11c⁺CD11b⁺ population were CD1c⁻ (Figure 3c), we expanded our phenotypical characterization to include CD163, known to be highly expressed on FRT macrophages[25]. However, CD163 was barely detectable in most of

the tissues (Figure 3f), suggesting that macrophages were not a major contaminating population.

Overall, these results demonstrate that *bona-fide* CD1c$^+$ myeloid DCs constitute a major population in both CD11b^{low} and CD11b$^+$ cells. However, the presence of CD14$^+$CD1c$^-$ cells that lack macrophage markers (CD163), likely indicate that the CD14$^+$ population represents a mixture of DCs and monocyte-derived cells.

HIV capture is mediated by CD11c$^+$CD14$^+$ cells in endometrium, endocervix and ectocervix

To evaluate the ability of different DC subsets to capture HIV, mixed cell suspensions were exposed to GFP-labeled HIV-viral-like particles (VLP) carrying R5Env proteins for 1h and then analyzed by flow cytometry. R5Env proteins were chosen based on the evidence that mucosal transmission occurs with HIV utilizing CCR5 coreceptor[26-28]. HIV-GFP VLP capture occured throughout the FRT, with no significant differences between anatomical sites (Figure 4a). Viral capture was detected exclusively on CD11c$^+$CD14$^+$ cells in EM, CX and ECX (Figure 4b, upper row), but not CD14$^-$ DCs or CD103$^+$ DCs (Figure 4b and 4c). Since the majority of HIV-GFP VLPs were captured by CD11c$^+$CD14$^+$ cells, we analyzed CD1c expression to further characterize the nature of the populations with viral capture potential. CD1c was expressed on approximately 20-30% of HIV-GFP VLP+ cells (Figure 4d), indicating that CD1c$^+$ myeloid DCs as well as CD11c$^+$CD14$^+$ monocyte-derived cells have the ability to capture HIV.

Next we explored if HIV capture was mediated by DC-SIGN$^+$ cells. As shown in figure 4e, DC-SIGN$^+$ as well as DC-SIGN$^-$ cells captured HIV-GFP VLP; however, within HIV-GFP VLP$^+$ cells, the predominant population with capture potential was DC-SIGN$^-$(Figure 4f, white circles). These results suggest that CD103$^+$ DCs and DC-SIGN$^+$ cellss are differentially involved in HIV acquisition, and that CD14$^+$CD1c$^+$ DCs with HIV capture potential are present throughout the FRT.

CD1a expression and maturation status of DCs in the FRT

To further characterize DCs in the FRT, we analyzed CD1a expression and maturation status of DCs in the different tissues. As seen in Figure 5a, CD11c$^+$ cells could be divided into 4 subsets according to CD1a and CD14 expression: i) CD1a$^+$CD14$^-$, ii) CD1a^{low}CD14^{low}, iii) CD1a$^-$CD14^{hi}, iv) CD1a$^-$CD14$^-$. Of these, CD1a^{low}CD14^{low} and CD1a$^-$CD14^{hi} were CD11b$^+$ DCs, CD1a$^+$CD14$^-$ expressed intermediate levels of CD11b and CD1a$^-$CD14$^-$ were CD11b^{low} DCs (Figure 5b). The same pattern was observed in EM, CX and ECX.

Next we assessed maturation status of the different DC subsets and found that HLA-DR and CD86 were expressed on all four subsets (not shown). Using CD83, a well-recognized marker for mature DCs, we found expression on more than 90% of CD1a$^+$CD14$^-$ DCs and about 35% of CD1a^{low}CD14^{low} DCs, with no CD83 detected on CD1a$^-$CD14^{hi} or CD1a$^-$CD14$^-$ DCs (Figure 5c; P<0.0001).

Upon maturation, DCs are known to up-regulate CCR7 which controls the migration of cells to secondary lymphoid organs for antigen presentation[29]. As seen in Figure 5d, CCR7 was negative or barely detectable on CD1a$^-$CD14^{hi} and CD1a$^-$CD14$^-$ DCs, in agreement with the

absence of CD83 and confirming immature DC state. CCR7 was expressed on CD1a^{low}CD14^{low} and CD1a$^+$CD14$^-$ DCs consistent with increased maturation. However, it is worth noting that CD1a$^+$CD14$^-$ DCs expressed low CCR7 levels relative to their CD83 expression compared to CD1a^{low}CD14^{low} DCs. No significant differences were found for CD83 or CCR7 expression between EM, CX and ECX for each subset (Supplementary Figure 2).

Isolation of DCs from the FRT using CD1a or CD14 positive magnetic bead selection

We developed a protocol to isolate a purified population of mucosal DCs using positive magnetic bead selection with either CD1a (Figure 6a, Top) or CD14 (Figure 6a, Bottom), to later evaluate anti-HIV responses by DCs from the FRT. As seen in Figure 6b, each protocol resulted in a majority of cells that were CD11c$^+$CD11b$^+$. CD1a$^+$ selection provided a homogeneous population with about 90% of selected cells expressing the HIV receptor CD4 and 80 % the coreceptor CCR5 (Figure 6c, Top). CD14$^+$ selected cells were more heterogeneous with approximately 65% of cells expressing CD4 and 70% CCR5 (Figure 6c, Bottom). Purity of the population and FMO controls are shown in supplementary figure 3e-f.

Selected cells showed dendritic morphology (Figure 6d). To further demonstrate that the magnetically selected cells contained a majority of DCs, their ability to stimulate naïve T cells was evaluated. After 6 days in co-culture, both mucosal CD1a and CD14 selected cells were able to induce proliferation of allogeneic naïve T cells (figure 6e). Proliferation levels were similar to those induced by *in vitro* generated monocyte-derived DCs (MoDCs) used as a control. These results indicate that a significant proportion of selected cells display DC functions.

Secretion of cytokines and chemokines by FRT DCs in response to HIV stimulation

To characterize the early responses to HIV by FRT DCs, CD14$^+$ selected cells from EM, CX and ECX were stimulated with HIV-BaL for 3h and secretions analyzed for the presence of a selected panel of cytokines and chemokines by luminex assay. To mimic mucosal transmission[26-28] HIV-BaL was selected as a well-defined CCR5 coreceptor utilizing HIV reference strain, given that low cell availability prevented us from using a panel of bona fide transmitted/founder strains.

As shown in Figure 7, CCL2 (MCP-1: 2 fold increase) and CCR5 ligands (CCL3: 2 fold increase and CCL4: 4 fold increase) were significantly up-regulated in response to HIV challenge. There was a modest but significant increase in IL-8 secretion (1.3 fold). In contrast, classical proinflammatory cytokines (IL-6, IL1β, TNFα) were not modified within 3h of viral exposure. Importantly, IFNα2, IL1α and IL-10 were undetectable or barely detectable before and after the 3h challenge. No significant differences were found between tissues, except for a trend towards higher constitutive production of these molecules in ECX relative to that seen in EM and CX.

Rapid secretion of antimicrobials by endometrial CD1a⁺ and CD14⁺ selected cells in response to HIV stimulation

To further evaluate the antiviral innate responses that occur immediately after mucosal DCs encounter HIV, we analyzed the secretion of antimicrobials by FRT DC. Purified $CD1a^+$ or $CD14^+$ cells from the EM were stimulated with HIV-BaL for 3h prior to secretion analysis for the presence of a range of antimicrobials with known anti-HIV activity. For these studies, we used a sensitive multiplex assay developed for simultaneous detection of diverse anti-HIV molecules in small volumes to allow studies with limited cell numbers[30]. Under these conditions, we were only able to recover $CD1a^+$ and $CD14^+$ cells from the endometrium in sufficient numbers to perform HIV stimulation studies.

Of seven antimicrobials tested, endometrial CD1a and CD14 selected cells constitutively produced elafin, CCL5 (RANTES), SLPI and CCL20 (MIP3α) (Figure 8a; black points). HBD2 and HBD3 were undetectable and lactoferrin could not be evaluated because of high background concentrations in the culture media (not shown). Following HIV stimulation, significant increases in secreted elafin (P<0.004), CCL5 (P<0.0008) and SLPI (P<0.004) were observed within 3h (Figure 8a; open points). However, when the same cells were maintained in culture for 21 additional hours following removal of the 3h conditioned media, differences were undetectable (Figure 8b), suggesting that the effects observed were due to rapid release of preformed molecules.

To determine whether $CD1a^+$ and $CD14^+$ cells responded similarly to HIV stimulation, we normalized the data according to cell number and compared baseline production of the different molecules (Figure 8c) and responses after HIV stimulation (Figure 8d). Compared to $CD14^+$ cells, baseline secretion of SLPI was significantly higher in CD1a selected cells (P=0.015) as well as a trend for greater CCL5 production (P=0.06), with no detectable differences for elafin or CCL20. Upon HIV exposure, compared to $CD14^+$ cells, $CD1a^+$ cells displayed a stronger up-regulation of elafin (3-fold vs 1.6-fold; P=0.016) and a trend for SLPI (1.9-fold vs 1.4-fold; P=0.06), but $CD1a^+$ and $CD14^+$ cells up-regulated CCL5 equally (6.8-fold vs 5.5-fold).

Since CD1a selected cells expressed more CCR5 than CD14 selected, we evaluated the contribution of CCR5 binding to antimicrobial release by using HIV-1-BaL gp120, to try to identify the mechanism triggering secretion. Selected cells were treated with gp120 for 3h, but no differences were found between treated and untreated cells, suggesting that the mechanism was not mediated through CCR5 (Figure 8e).

E₂ suppresses HIV stimulated secretion of elafin and SLPI

Recognizing that E_2 modulates innate immune responses in monocyte-derived DCs[16,17], we evaluated the potential effects of E_2 on mucosal DC anti-HIV responses. Isolated DCs were pretreated with E_2 overnight (24h) and then exposed to HIV for 3h. As shown in Figure 9, pre-treatment of the cells with E_2 prevented the induction of elafin and SLPI that was observed in the absence of E_2 (P=0.01). In contrast, CCL5 was still significantly up-regulated in the presence of E_2 (P=0.01), although with reduced secretion levels. No effects were observed for CCL20 (not shown).

Discussion

In the present study, direct comparison of DC subsets from human endometrium, endocervix and ectocervix demonstrates that: 1) DCs at each anatomical site display unique cell phenotypes; 2) DCs with the ability to capture HIV display a specific phenotype (CD14^{+} CD103^{-}) and are present throughout the FRT and 3) HIV exposure induces rapid release of chemokines and innate anti-HIV molecules by FRT DCs. To the best of our knowledge, this study is the first to comprehensively analyze and compare DCs from different anatomical compartments in the FRT. Since HIV can reach all the anatomical regions of the FRT, characterization of the DCs present at each site of HIV entry is basic information necessary for the development of preventive vaccines and microbicides.

A main conclusion in our study is that the majority of DCs present throughout the FRT are CD11b^{+}CD14^{+}. This finding was unexpected considering that conventional DCs are regarded as CD14^{-} cells based on studies with blood DCs[31]. CD14^{+} DCs have been described in human skin, where they are involved in the development of antibody responses[32], and in the human vagina, where they have the ability to polarize naïve CD4^{+} T cells toward Th1 in vitro[18]. The present study extends these findings by demonstrating that CD14^{+} DCs are the main resident DC population at all mucosal FRT sites analyzed and that they may be relevant for HIV capture as discussed below.

There is on-going controversy as to whether CD14^{+} DCs represent bona-fide DCs or monocyte-derived cell with high plasticity able to display DC or macrophage functions[33]. In our study, the majority of CD11c^{hi}CD11b^{+}CD14^{+} cells co-expressed CD1c (myeloid DC marker) and lacked CD163 expression (macrophage marker). In addition, we demonstrate induction of naïve T cell proliferation by mucosal CD14^{+} selected cells, a unique characteristic of DCs. These results are consistent with populations of CD1c^{+}CD14^{+} cells found in the vagina[18] and likely represent an example of the critical influence of the mucosal environment on DC differentiation[33]. Nevertheless, the large numbers of CD14^{+}CD1c^{-} cells also found in our study, likely indicate that the CD14^{+} population represents a mixture of DCs and monocyte-derived cells. Further investigation is needed to address this issue.

Another major finding of our study, is the fundamental difference in DC phenotype between EM, CX and ECX. The most striking difference regarding phenotype was that CD103^{+} DCs were found selectively in the EM. To the best of our knowledge, this is the first time that CD103^{+} DCs have been identified in human endometrium. Others have reported the absence of CD103^{+} DCs in ECX and vagina[18,20] but here, by performing side-by-side comparisons, we were able to characterize these cells in the human EM. This selective distribution is likely dependent on the mucosal environment since different studies demonstrate that local production of GM-CSF regulates CD103 expression on murine DCs[22]. In this context, the preferential presence of CD103^{+} DCs in the EM could be partially explained by increased GM-CSF production by endometrial epithelial cells relative to that seen with cervical epithelial cells[34]. Of note, we observed that T cells from the same donors expressed equivalent levels of CD103 among tissues, suggesting that CD103 expression on DCs and T cells is regulated by different mechanisms in the FRT.

The function of CD103^{+} DCs in the human endometrium remains to be determined. In the human intestine, CD103^{+} DCs represent a critical subset for the induction of regulatory T cells and oral tolerance in the steady state[35,36]. Additionally, murine models demonstrate that hepatic and pulmonary CD103^{+} DCs are required for the induction of CD8^{+} T cell responses to viral infections[37,38]. Interestingly, pulmonary CD103^{+} DCs are specialized in the capture and presentation of antigens derived from apoptotic cells[39]. A recent study also demonstrated that murine endometrial CD103^{+} DCs promote T regulatory cell proliferation in response to inactivated *Chlamydia trachomatis*[40]. Whether human endometrial CD103^{+} DCs play a role in inducing regulatory responses, presentation of apoptotic cell-derived antigens or CD8 T cell responses to viral infections remains to be determined. The differential distribution of CD103^{+} DCs we found between EM, CX and ECX is consistent with the need for tolerance and induction of regulatory T cell responses in the endometrium, the site of implantation and gestation, both prior to and during pregnancy. Interestingly, we recently demonstrated that Th17 cells were significantly reduced in the EM compared to CX and ECX[6]. If endometrial CD103^{+} DCs drive naïve T cells to become regulatory T cells instead of Th17 cells, the selective presence of this DC population in the EM could be related to the relative absence of Th17 cells. The present studies begin to unravel the very unique immune cell environment in the EM.

Another profound phenotypical difference found in our study involved DC-SIGN expression. In contrast to CD103, DC-SIGN[+] DCs were identified in the three anatomical sites analyzed. DC-SIGN[+] DCs have been previously described by different studies in cervix and vagina[19,20,41,42]. Unlike other studies, our studies with matched tissues from the same patient indicate that DC-SIGN expression was significantly higher on DCs in the endocervix compared to endometrium and ectocervix. Previous studies from our group demonstrated that TGF-β present in conditioned media from endometrial epithelial cells was able to down-regulate DC-SIGN expression on monocyte-derived DCs[43]. These findings suggest that decreased DC-SIGN expression observed on endometrial DCs in the present study could be due to the effect of TGF-β present in the endometrial environment. We also observed expression of CD207 (langerin) only on CD1c^{+} DCs and preferentially in the EM. A recent study demonstrated that TGF-β is also responsible for up-regulation of CD207 (Langerin) on CD1c^{+} DCs and that these cells are different from Langerhans Cells[24].

Our studies demonstrate that CD14^{+}CD103^{-} cells display HIV capture potential, and that within the cells that capture the virus, about 30% were CD1c^{+} myeloid DCs throughout the FRT. These results suggest that the EM, in addition to the CX and ECX, is a potential site for HIV-acquisition. Even though CD4^{+} T cells in the EM are poorly susceptible to HIV-infection[6], the presence of DCs with the ability to capture virus and potentially migrate and infect CD4^{+} T cells in the regional lymph nodes suggests an under-appreciated uterine portal of entry for HIV and viral dissemination. Unexpectedly, we found that while some DCs expressed DC-SIGN, the majority that captured HIV did not express DC-SIGN. Further, the increased presence of DC-SIGN[+] DCs in endocervix did not correlate with increased viral capture in this anatomical site. Our results are in agreement with a previous report showing that HIV internalization by vaginal Langerhans cells was only marginally reduced after blockade of C-type lectin receptors[3]. The importance of DC-SIGN in HIV capture and trans-infection of T cells has been demonstrated previously using monocyte-derived DCs and

primary DC-SIGN[+] DCs from rectum and skin[44-47], but studies comparing primary DC-SIGN[+] DCs from different FRT sites were lacking until now. Moreover, these results suggest that receptors other than DC-SIGN may be involved in HIV acquisition in the FRT.

In the present study we demonstrate that resident DCs in the FRT mucosa can be found with different levels of maturation. We found that HLA-DR expression was highest on ectocervical DCs, suggesting an increased general maturation status, perhaps mediated by the larger microbial load known to be present in the lower FRT. While we did not perform migration and trans-infection assays, based on studies by others demonstrating that CCR7 is involved in cell migration to lymph nodes, and that CD1c^{+} DCs are migratory, we speculate that a proportion of the DCs that capture HIV in the FRT have the potential to transport virus to lymphoid tissues. However, we cannot exclude the possibility that movement may be to adjacent sites in the reproductive tract rich in lymphoid aggregates[48]. It is worth noting that the expression levels of CCR7 in FRT DCs found in the present study were low compared to those reported by others in the intestinal tract[23]. This could reflect that DCs in the FRT may have impaired or limited migration potential to lymph nodes or that this function is under tighter control in the FRT[49]. Conversely, another portion of the cells that captured the virus, which lack CCR7 expression (i.e. CD14^{hi}), would remain in the tissue and potentially contribute to local infection. Further studies are needed to evaluate migration and HIV trans-infection properties of specific FRT DC subsets. Even though CD14^{-} DCs are not involved in direct viral capture, their role in HIV acquisition deserves further investigation, since we demonstrate that they are responsive to HIV stimulation as discussed below. Future studies will address this issue and the implications for HIV acquisition and dissemination.

Our study demonstrates that in response to HIV, within 3h, mucosal DCs secrete CCR5-ligands and other chemokines (CCL2, IL-8) and a spectrum of innate anti-HIV molecules, but not the classical pro-inflammatory cytokines, IFN-α2 or IL-10. Studies until now have focused on intracellular innate immune pathways or analyzed later time points after HIV exposure of monocyte-derived DCs, so these acute responses have been missed. We demonstrate for the first time that elafin and SLPI are constitutively expressed in FRT DCs, and that in response to HIV exposure, both are rapidly secreted along with CCR5 ligands and other chemokines. Our findings that DCs in the FRT secrete SLPI and elafin, which are anti-proteases with anti-inflammatory and chemoattractant properties[50], indicate an additional level of protection against HIV acquisition that is not widely recognized. Both molecules display anti-HIV activity in vitro by actions on target cells[51,52] or direct viral inactivation[53] for SLPI and elafin respectively. Furthermore, the presence of SLPI and elafin in genital secretions is associated with protection against HIV-acquisition[54,55]. In contrast, the presence of CCL5 in genital secretions has been associated with increased HIV acquisition[54] despite its demonstrated anti-HIV activity in vitro, possibly due to chemoattraction of CCR5^{+} CD4^{+} T cells, the most HIV-susceptible target cells present in the human FRT as reported previously by others and us[6,9,56-59]. Therefore, whether the secretion levels of the different chemokines, elafin and SLPI found in the present study would primarily serve an anti-HIV, anti-inflammatory or cell recruitment function *in vivo* is difficult to predict.

Previous studies using monocyte-derived DCs demonstrated that HIV specifically inhibits innate immune responses (interferon production), establishing the concept that HIV dampens innate immunity in DCs to facilitate infection[60,61]. Our results with mucosal DCs complement this information by showing that secreted innate immunity is triggered rapidly in response to viral exposure. Therefore, innate alarms and cascades for activation of surrounding cells and/or recruitment of target cells to the site of viral entry are already in place before suppression of other innate responses takes place.

We found that the rapid anti-viral response of DCs was suppressed by pretreatment with E_2, specifically the anti-inflammatory component of the response (i.e. elafin and SLPI). This suppressive activity could result in either decreased or increased susceptibility to HIV acquisition. The mechanisms that could increase HIV acquisition would be decreased secretion of SLPI and elafin, with consequent reduced anti-HIV activity, or increased mucosal activation due to reduction of the anti-inflammatory component of the response. Immune activation has been shown in SLPI knockout mice whose DCs release more proinflammatory cytokines and induce enhanced proliferation of T cells[62]. Alternatively, the mechanism for decreased risk of infection after reduced SLPI and elafin production by E_2 could be due to decreased target cell recruitment. How important each of these components will be in the overall response remains to be elucidated. Consistent with the suppressive effect of E_2 observed here, a previous study demonstrated decreased α-defensins 1-3 production by blood DCs in response to E_2 treatment, but not to progesterone (P)[16]. While P effects were not addressed here due to limited cell numbers, the roles that P and E_2/P in combination may play in anti-HIV responses deserves further investigation considering the multiple studies suggesting that high levels of P increase susceptibility to HIV infection[9-11,63].

In conclusion we demonstrate that DCs in the different anatomical compartments of the FRT are phenotypically distinct with differential viral capture properties, but they all rapidly respond to HIV with innate secreted molecules. Our results are relevant for rational design of microbicides and vaccines to prevent sexual transmission of HIV.

Methods

Study subjects

Written informed consent was obtained before surgery from HIV-negative women undergoing hysterectomies at Dartmouth-Hitchcock Medical Center (Lebanon, NH). Studies were approved by Dartmouth College Institutional Review Board and the Committee for the Protection of Human Subjects (CPHS). Surgery was performed to treat benign conditions including fibroids, prolapse and menorraghia. Hormonal contraceptives were not administered before surgery. Trained pathologists selected tissue samples from endometrium (EM), endocervix (CX) and ectocervix (ECX) free of pathological lesions and distant from the sites of pathology. Women were HIV- and HPV- but no additional information regarding other genital infections was available. Characteristics of the women included in the study are shown in Table 1.

Tissue processing

Matched tissues from the EM, CX and ECX of the same patient were used for all experiments, except for antimicrobial production studies in response to HIV stimulation, for which enough cells could only be isolated from the EM. In some cases, only endometrial tissue was provided by pathology. Vaginal tissues were not available. Tissues were processed to obtain a stromal cell suspension as described previously[6], using 0.05% collagenase type IV (Sigma-Aldrich, St. Louis, MO) and 0.01% DNAse (Worthington Biochemical, Lakewood, NJ). After filtering through a 20μm mesh screen (Small Parts) to separate epithelial cells from stromal cells, stromal cells were further purified by standard Ficoll density gradient centrifugation to remove dead cells and enrich the immune cell population before further purification. Cell preparations underwent dead cell removal (Dead Cell Removal Kit, Miltenyi biotech) as described[6], resulting in more than 90% cell viability by trypan blue staining. After dead cell removal, mixed cell suspensions were used for phenotypical analyses.

Flow cytometry

Mixed cell suspensions were stained for surface markers with combinations of the following antibodies: CD45-vioblue450, CD11b-PE (Tonbo, San Diego, CA), CD11c-APC, CCR5-PE-Cy7 (BD Biosciences, San Jose, CA), CCR7-PE-Cy7, HLA-DR-FITC, CD3-VioGreen (Miltenyi Biotec), CD3-APC, CD11c-PerCp-Cy5.5, CD1c-PE-dazzle, CD163-APC, HLA-DR-BV570, CD207-APC, CD1a AF700 (Biolegend), CD103-PE-Cy7, CD83-PE, CD14-e780, CD1a-FITC, CD86-e710 (eBiosciences, San Diego, CA), DC-SIGN-FITC, DC-SIGN-PE, DC-SIGN-APC (R&D systems, Minneapolis, MN). Dead cells were excluded with 7AAD (Southern Biotech) or zombie dye yellow staining (Biolegend). Analysis was performed on 8-color MACSQuant 10 (Miltenyi biotech) or Gallios (Beckman Coulter) flow cytometers and data analyzed with FlowJo software (Tree Star, Inc. Ashland, OR). Expression of surface markers is shown as percentage of positive cells. Fluorescence minus one (FMO) strategy was used to establish appropriate gates. The gating strategy is shown in supplementary Figure 1.

Generation of GFP-labeled Virus-like particles

A modified pNL4-3 provirus-based plasmid for expression of GFP-labelled virus like particles (VLP) and encoding NL4-3 Env *in cis*, (referred to as K795) was described previously[64]. Briefly, the EGFP coding sequence is expressed in frame at the 3′ end of gag, replacing the protease and most of reverse transcriptase coding region. In addition, a plasmid in which the env orf was inactivated, and from which no functional Env is expressed (referred to as K806) was derived from K795 for pseudotyping, and complemented with pBaL.26 Env expression plasmid (NIH AIDS Reagent program, Catalog Number 11446, contributed by Dr. John Mascola)[65]. Virus-like particles which are EGFP-labeled and non-infectious were produced by transfection, concentrated by ultracentrifugation and enumerated essentially as described[64].

Viral capture assay

Mixed cell suspensions were incubated with HIV-GFP viral like particles (VLPs) carrying R5env proteins at a concentration of 10,000 VLPs/cell for 1h at 37 °C. Following incubation cells were washed to remove unbound VLPs and stained for flow cytometric analysis.

CD14$^+$ and CD1a$^+$ cell isolation and morphology

Following ficoll purification, DCs were isolated using positive magnetic bead selection with either the CD14$^+$ or CD1a$^+$ isolation kits (Miltenyi Biotec) according to the manufacturer's instructions. After two rounds of positive selection, purity of the CD14$^+$ and CD1a$^+$ population was about 90% (see Supplementary Figure 3e). Isolated DCs were plated (20,000-100,000 cells/well) in round bottom ultra-low attachment 96-well plates (Corning, Corning, NY) in Xvivo15 without Phenol Red (Invitrogen) supplemented with 1% charcoal dextran-stripped human AB serum (Valley Biomedical) for in-vitro stimulation with HIV and hormones (E$_2$). No changes in phenotypic markers were observed after bead selection, except for a small decrease in CD14 MFI (Supplementary Figure 3c-d). The rate of cell recovery per gram of tissue after magnetic selection is shown in supplementary Figure 3a-b.

Cell morphology was evaluated after cytospin and Giemsa staining of CD1a and CD14 selected cells. Images were acquired using a IX73 Inverted Microscope (Olympus) with a 40× objective.

Allogeneic naïve T cell stimulation assay

Blood naïve T cells were purified after ficoll gradient using the Naïve Pan T Cell Isolation Kit (Miltenyi Biotec) and stained with Cell Proliferation Dye eFluor-670 (eBioscience) as recommended by the manufacturer. Purified mucosal CD1a+ or CD14+ were plated with naïve T cells (1:15) in round-bottom 96-well plates, in Xvivo 15 media (Invitrogen) supplemented with 10% human AB serum (Valley Biomedical). After 6 days in culture, proliferation of T cells was assessed by flow cytometry after staining with zombie yellow dye (Biolegend) and CD3-APC-Cy7 (Tonbo). As a control, blood monocyte-derived DC were generated in vitro with IL-4 and GM-CSF[66] after CD14+ selection as previously described[16].

Hormone treatment

Immediately after isolation, CD14$^+$ or CD1a$^+$ selected cells were treated with 17β-estradiol (E$_2$; Sigma) for 24h and washed before HIV exposure. E$_2$ was dissolved in 100% ethanol at an initial concentration of 1×10^{-3}M prior to evaporation to dryness and resuspension in Xvivo 15 without Phenol Red (Invitrogen) media containing 1% of charcoal dextran-stripped human AB serum (Valley Biomedical) to a E$_2$ concentration of 1×10^{-5}M. Dilutions were made to achieve a final working hormone concentration of 5×10^{-8}M. As a control, an equivalent amount of 100% ethanol without dissolved hormone was initially evaporated. All control conditions contained evaporated ethanol as a control. Because dextran charcoal treatment of serum may introduce LPS contamination, expression of costimulatory molecules after incubation of cells with or without 1% charcoal-stripped human AB serum was assessed (supplementary figure 2c).

HIV and gp120 stimulation

HIV-1-BaL (R5) isolates were obtained from the AIDS Research and Reference Reagent Program, Division of AIDS, NIAID, NIH, from Dr. Suzanne Gartner, Dr. Mikulas Popovic and Dr. Robert Gallo[67] and propagated as described[13]. Purified CD1a+ or CD14+ DCs were treated with HIV-1 BaL for 3h at a MOI of 0.5 or with 1 μg/ml of gp120 protein derived from HIV-1-BaL (NIH AIDS Reagent Program, Division of AIDS, NIAID, NIH) after which the culture supernatants were collected and stored at -80°C until antimicrobial analysis. Media was replaced and cells kept in culture for 21 more hours after which cell supernatants were collected for antimicrobial analysis. Uninfected controls were incubated for the same length of time in media without virus or gp120.

Luminex assay

Cytokines and chemokines were measured using Millipore human cytokine multiplex kits (EMD Millipore. Corporation, Billerica, MA) according to the instructions. Signal was measured using the Bio-Plex array reader. Bio-Plex Manager software with five-parametric-curve fitting was used for data analysis. Molecules measured included: IFN-α2, IL-10, IL-1α, IL-1β, IL-6, IL-8, CCL2 (MCP-1), CCL3 (MIP-1α), CCL4 (MIP-1β) and TNF-α.

Multiplex assay

7 different molecules known to have anti-HIV activity were evaluated in culture supernatants using a custom microsphere multiplex assay described previously[30]. Briefly, commercially available antibody pairs were alternatively coupled to fluorescently-coded magnetic beads to capture analyte or PE-functionalized for detection of HBD2, HBD3, elafin, SLPI, CCL5 (RANTES), CCL20 and lactoferrin. Samples were inactivated with TRITON X100, diluted 1:3 before analysis and run in triplicate.

Statistics

Data analysis was performed using the GraphPad Prism 5.0 software. A two sided P-value <0.05 was considered statistically significant. Comparison of two groups was performed with the non-parametric U-Mann Whitney test or Wilcoxon paired test. Comparison of three or more groups was performed applying the non-parametric Kruskal-Wallis or the paired Friedmann test followed by Dunns post-test. Data are represented as the median ± interquartile range (IQR).

Supplementary Material

Refer to Web version on PubMed Central for supplementary material.

Acknowledgments

References

1. WHO. Progress report 2011: Global HIV/AIDS response. 2011. http://www.who.int/hiv/pub/progress_report2011/en/index.html

2. Nazli A, et al. Exposure to HIV-1 directly impairs mucosal epithelial barrier integrity allowing microbial translocation. PLoS Pathog. 2010; 6:e1000852. [PubMed: 20386714]

3. Hladik F, et al. Initial events in establishing vaginal entry and infection by human immunodeficiency virus type-1. Immunity. 2007; 26:257–270. doi:S1074-7613(07)00134-3[pii]10.1016/j.immuni.2007.01.007. [PubMed: 17306567]

4. Wu L, KewalRamani VN. Dendritic-cell interactions with HIV: infection and viral dissemination. Nat Rev Immunol. 2006; 6:859–868. doi:nri1960[pii]10.1038/nri1960. [PubMed: 17063186]

5. Wira CR, Rodriguez-Garcia M, Patel MV. The role of sex hormones in immune protection of the female reproductive tract. Nat Rev Immunol. 2015; 15:217–230. DOI: 10.1038/nri3819 [PubMed: 25743222]

6. Rodriguez-Garcia M, Barr FD, Crist SG, Fahey JV, Wira CR. Phenotype and susceptibility to HIV infection of CD4+ Th17 cells in the human female reproductive tract. Mucosal Immunol. 2014; 7:1375–1385. DOI: 10.1038/mi.2014.26 [PubMed: 24759207]

7. Sallusto F, Zielinski CE, Lanzavecchia A. Human Th17 subsets. Eur J Immunol. 2012; 42:2215–2220. DOI: 10.1002/eji.201242741 [PubMed: 22949319]

8. Tagliani E, Erlebacher A. Dendritic cell function at the maternal-fetal interface. Expert review of clinical immunology. 2011; 7:593–602. DOI: 10.1586/eci.11.52 [PubMed: 21895472]

9. Saba E, et al. Productive HIV-1 infection of human cervical tissue ex vivo is associated with the secretory phase of the menstrual cycle. Mucosal Immunol. 2013

10. Vishwanathan SA, et al. High susceptibility to repeated, low-dose, vaginal SHIV exposure late in the luteal phase of the menstrual cycle of pigtail macaques. J Acquir Immune Defic Syndr. 2011; 57:261–264. DOI: 10.1097/QAI.0b013e318220ebd3 [PubMed: 21546848]

11. Kersh EN, et al. SHIV susceptibility changes during the menstrual cycle of pigtail macaques. Journal of medical primatology. 2014; 43:310–316. DOI: 10.1111/jmp.12124 [PubMed: 24779484]

12. Asin SN, Heimberg AM, Eszterhas SK, Rollenhagen C, Howell AL. Estradiol and progesterone regulate HIV type 1 replication in peripheral blood cells. AIDS research and human retroviruses. 2008; 24:701–716. DOI: 10.1089/aid.2007.0108 [PubMed: 18462082]

13. Rodriguez-Garcia M, et al. Estradiol Reduces Susceptibility of CD4(+) T Cells and Macrophages to HIV-Infection. PLoS One. 2013; 8:e62069. [PubMed: 23614015]

14. Tasker C, et al. 17beta-estradiol protects primary macrophages against HIV infection through induction of interferon-alpha. Viral Immunol. 2014; 27:140–150. DOI: 10.1089/vim.2013.0120 [PubMed: 24801776]

15. Szotek EL, Narasipura SD, Al-Harthi L. 17beta-Estradiol inhibits HIV-1 by inducing a complex formation between beta-catenin and estrogen receptor alpha on the HIV promoter to suppress HIV transcription. Virology. 2013; 443:375–383. DOI: 10.1016/j.virol.2013.05.027 [PubMed: 23769242]

16. Escribese MM, et al. Alpha-defensins 1-3 release by dendritic cells is reduced by estrogen. Reprod Biol Endocrinol. 2011; 9:118. doi:1477-7827-9-118[pii]10.1186/1477-7827-9-118. [PubMed: 21861873]

17. Escribese MM, et al. Estrogen inhibits dendritic cell maturation to RNA viruses. Blood. 2008; 112:4574–4584. DOI: 10.1182/blood-2008-04-148692 [PubMed: 18802009]

18. Duluc D, et al. Functional diversity of human vaginal APC subsets in directing T-cell responses. Mucosal Immunol. 2013; 6:626–638. DOI: 10.1038/mi.2012.104 [PubMed: 23131784]

19. Shen R, et al. Vaginal myeloid dendritic cells transmit founder HIV-1. J Virol. 2014; 88:7683–7688. DOI: 10.1128/JVI.00766-14 [PubMed: 24741097]

20. Trifonova RT, Lieberman J, van Baarle D. Distribution of immune cells in the human cervix and implications for HIV transmission. Am J Reprod Immunol. 2014; 71:252–264. DOI: 10.1111/aji.12198 [PubMed: 24410939]

21. Bogunovic M, Mortha A, Muller PA, Merad M. Mononuclear phagocyte diversity in the intestine. Immunologic research. 2012; 54:37–49. DOI: 10.1007/s12026-012-8323-5 [PubMed: 22562804]

22. Merad M, Sathe P, Helft J, Miller J, Mortha A. The dendritic cell lineage: ontogeny and function of dendritic cells and their subsets in the steady state and the inflamed setting. Annu Rev Immunol. 2013; 31:563–604. DOI: 10.1146/annurev-immunol-020711-074950 [PubMed: 23516985]

23. Mann ER, et al. Compartment-specific immunity in the human gut: properties and functions of dendritic cells in the colon versus the ileum. Gut. 2015

24. Bigley V, et al. Langerin-expressing dendritic cells in human tissues are related to CD1c+ dendritic cells and distinct from Langerhans cells and CD141high XCR1+ dendritic cells. J Leukoc Biol. 2015; 97:627–634. DOI: 10.1189/jlb.1HI0714-351R [PubMed: 25516751]

25. Jensen AL, et al. A subset of human uterine endometrial macrophages is alternatively activated. Am J Reprod Immunol. 2012; 68:374–386. DOI: 10.1111/j.1600-0897.2012.01181.x [PubMed: 22882270]

26. Saba E, et al. HIV-1 sexual transmission: early events of HIV-1 infection of human cervico-vaginal tissue in an optimized ex vivo model. Mucosal Immunol. 2010; 3:280–290. DOI: 10.1038/mi. 2010.2mi20102[pii] [PubMed: 20147895]

27. van't Wout AB, et al. Macrophage-tropic variants initiate human immunodeficiency virus type 1 infection after sexual, parenteral, and vertical transmission. The Journal of clinical investigation. 1994; 94:2060–2067. DOI: 10.1172/JCI117560 [PubMed: 7962552]

28. Zhu T, et al. Genotypic and phenotypic characterization of HIV-1 patients with primary infection. Science. 1993; 261:1179–1181. [PubMed: 8356453]

29. Randolph GJ, Angeli V, Swartz MA. Dendritic-cell trafficking to lymph nodes through lymphatic vessels. Nat Rev Immunol. 2005; 5:617–628. DOI: 10.1038/nri1670 [PubMed: 16056255]

30. Boesch AW, et al. A multiplexed assay to detect antimicrobial peptides in biological fluids and cell secretions. Journal of immunological methods. 2013; 397:71–76. DOI: 10.1016/j.jim.2013.09.001 [PubMed: 24035708]

31. Collin M, McGovern N, Haniffa M. Human dendritic cell subsets. Immunology. 2013; 140:22–30. DOI: 10.1111/imm.12117 [PubMed: 23621371]

32. Klechevsky E, Banchereau J. Human dendritic cells subsets as targets and vectors for therapy. Annals of the New York Academy of Sciences. 2013; 1284:24–30. DOI: 10.1111/nyas.12113 [PubMed: 23651190]

33. Schlitzer A, McGovern N, Ginhoux F. Dendritic cells and monocyte-derived cells: Two complementary and integrated functional systems. Seminars in cell & developmental biology. 2015; 41:9–22. DOI: 10.1016/j.semcdb.2015.03.011 [PubMed: 25957517]

34. Fahey JV, Schaefer TM, Channon JY, Wira CR. Secretion of cytokines and chemokines by polarized human epithelial cells from the female reproductive tract. Hum Reprod. 2005; 20:1439–1446. DOI: 10.1093/humrep/deh806 [PubMed: 15734755]

35. Jaensson E, et al. Small intestinal CD103+ dendritic cells display unique functional properties that are conserved between mice and humans. J Exp Med. 2008; 205:2139–2149. DOI: 10.1084/jem. 20080414 [PubMed: 18710932]

36. Coombes JL, Powrie F. Dendritic cells in intestinal immune regulation. Nat Rev Immunol. 2008; 8:435–446. DOI: 10.1038/nri2335 [PubMed: 18500229]

37. Kim TS, Braciale TJ. Respiratory dendritic cell subsets differ in their capacity to support the induction of virus-specific cytotoxic CD8+ T cell responses. PLoS One. 2009; 4:e4204. [PubMed: 19145246]

38. Krueger PD, Kim TS, Sung SS, Braciale TJ, Hahn YS. Liver-resident CD103+ dendritic cells prime antiviral CD8+ T cells in situ. J Immunol. 2015; 194:3213–3222. DOI: 10.4049/jimmunol. 1402622 [PubMed: 25712214]

39. Desch AN, et al. CD103+ pulmonary dendritic cells preferentially acquire and present apoptotic cell-associated antigen. J Exp Med. 2011; 208:1789–1797. DOI: 10.1084/jem.20110538 [PubMed: 21859845]

40. Stary G, et al. VACCINES. A mucosal vaccine against Chlamydia trachomatis generates two waves of protective memory T cells. Science. 2015; 348:aaa8205. [PubMed: 26089520]

41. Jameson B, et al. Expression of DC-SIGN by dendritic cells of intestinal and genital mucosae in humans and rhesus macaques. J Virol. 2002; 76:1866–1875. [PubMed: 11799181]

42. Duluc D, et al. Dendritic cells and vaccine design for sexually-transmitted diseases. Microbial pathogenesis. 2013; 58:35–44. DOI: 10.1016/j.micpath.2012.11.010 [PubMed: 23201532]

43. Ochiel DO, et al. Uterine epithelial cell regulation of DC-SIGN expression inhibits transmitted/ founder HIV-1 trans infection by immature dendritic cells. PLoS One. 2010; 5:e14306. [PubMed: 21179465]

44. Gurney KB, et al. Binding and transfer of human immunodeficiency virus by DC-SIGN+ cells in human rectal mucosa. J Virol. 2005; 79:5762–5773. DOI: 10.1128/JVI.79.9.5762-5773.2005 [PubMed: 15827191]

45. Reece JC, et al. HIV-1 selection by epidermal dendritic cells during transmission across human skin. J Exp Med. 1998; 187:1623–1631. [PubMed: 9584140]

46. de Witte L, Nabatov A, Geijtenbeek TB. Distinct roles for DC-SIGN+-dendritic cells and Langerhans cells in HIV-1 transmission. Trends in molecular medicine. 2008; 14:12–19. DOI: 10.1016/j.molmed.2007.11.001 [PubMed: 18055263]

47. Cavarelli M, Foglieni C, Rescigno M, Scarlatti G. R5 HIV-1 envelope attracts dendritic cells to cross the human intestinal epithelium and sample luminal virions via engagement of the CCR5. EMBO molecular medicine. 2013; 5:776–794. DOI: 10.1002/emmm.201202232 [PubMed: 23606583]

48. Yeaman GR, et al. Unique CD8+ T cell-rich lymphoid aggregates in human uterine endometrium. J Leukoc Biol. 1997; 61:427–435. [PubMed: 9103229]

49. Collins MK, Tay CS, Erlebacher A. Dendritic cell entrapment within the pregnant uterus inhibits immune surveillance of the maternal/fetal interface in mice. The Journal of clinical investigation. 2009; 119:2062–2073. DOI: 10.1172/JCI38714 [PubMed: 19546507]

50. Drannik AG, Henrick BM, Rosenthal KL. War and peace between WAP and HIV: role of SLPI, trappin-2, elafin and ps20 in susceptibility to HIV infection. Biochemical Society transactions. 2011; 39:1427–1432. DOI: 10.1042/BST0391427 [PubMed: 21936827]

51. McNeely TB, et al. Secretory leukocyte protease inhibitor: a human saliva protein exhibiting anti-human immunodeficiency virus 1 activity in vitro. The Journal of clinical investigation. 1995; 96:456–464. DOI: 10.1172/JCI118056 [PubMed: 7615818]

52. McNeely TB, et al. Inhibition of human immunodeficiency virus type 1 infectivity by secretory leukocyte protease inhibitor occurs prior to viral reverse transcription. Blood. 1997; 90:1141–1149. [PubMed: 9242546]

53. Ghosh M, et al. Trappin-2/Elafin: a novel innate anti-human immunodeficiency virus-1 molecule of the human female reproductive tract. Immunology. 2010; 129:207–219. DOI: 10.1111/j.1365-2567.2009.03165.x [PubMed: 19824918]

54. Morrison C, et al. Cervical inflammation and immunity associated with hormonal contraception, pregnancy, and HIV-1 seroconversion. J Acquir Immune Defic Syndr. 2014; 66:109–117. DOI: 10.1097/QAI.0000000000000103 [PubMed: 24413042]

55. Gonzalez SM, et al. High Expression of Antiviral Proteins in Mucosa from Individuals Exhibiting Resistance to Human Immunodeficiency Virus. PLoS One. 2015; 10:e0131139. [PubMed: 26091527]

56. Joag VR, et al. Identification of preferential CD4 T-cell targets for HIV infection in the cervix. Mucosal Immunol. 2015

57. Kaul R, et al. Genital levels of soluble immune factors with anti-HIV activity may correlate with increased HIV susceptibility. AIDS. 2008; 22:2049–2051. DOI: 10.1097/QAD.0b013e328311ac65 [PubMed: 18784472]

58. McKinnon LR, et al. Characterization of a human cervical CD4+ T cell subset coexpressing multiple markers of HIV susceptibility. J Immunol. 2011; 187:6032–6042. doi:jimmunol. 1101836[pii]10.4049/jimmunol.1101836. [PubMed: 22048765]

59. Rodriguez-Garcia M, Patel MV, Wira CR. Innate and adaptive anti-HIV immune responses in the female reproductive tract. J Reprod Immunol. 2013; 97:74–84. DOI: 10.1016/j.jri.2012.10.010S0165-0378(12)00645-6[pii] [PubMed: 23432874]

60. Harman AN, et al. HIV infection of dendritic cells subverts the IFN induction pathway via IRF-1 and inhibits type 1 IFN production. Blood. 2011; 118:298–308. DOI: 10.1182/blood-2010-07-297721 [PubMed: 21411754]

61. Harman AN, et al. HIV Blocks Interferon Induction in Human Dendritic Cells and Macrophages by Dysregulation of TBK1. J Virol. 2015; 89:6575–6584. DOI: 10.1128/JVI.00889-15 [PubMed: 25855743]

62. Samsom JN, et al. Secretory leukoprotease inhibitor in mucosal lymph node dendritic cells regulates the threshold for mucosal tolerance. J Immunol. 2007; 179:6588–6595. [PubMed: 17982048]

63. Wira CR, Fahey JV. A new strategy to understand how HIV infects women: identification of a window of vulnerability during the menstrual cycle. AIDS. 2008; 22:1909–1917. DOI: 10.1097/QAD.0b013e3283060ea400002030-200810010-00002[pii] [PubMed: 18784454]

64. Forthal DN, et al. IgG2 inhibits HIV-1 internalization by monocytes, and IgG subclass binding is affected by gp120 glycosylation. AIDS. 2011; 25:2099–2104. DOI: 10.1097/QAD.0b013e32834b64bd [PubMed: 21832933]

65. Li Y, et al. Characterization of antibody responses elicited by human immunodeficiency virus type 1 primary isolate trimeric and monomeric envelope glycoproteins in selected adjuvants. J Virol. 2006; 80:1414–1426. DOI: 10.1128/JVI.80.3.1414-1426.2006 [PubMed: 16415019]

66. Rodriguez-Garcia M, et al. Increased alpha-defensins 1-3 production by dendritic cells in HIV-infected individuals is associated with slower disease progression. PLoS One. 2010; 5:e9436. [PubMed: 20195543]

67. Gartner S, et al. The role of mononuclear phagocytes in HTLV-III/LAV infection. Science. 1986; 233:215–219. [PubMed: 3014648]
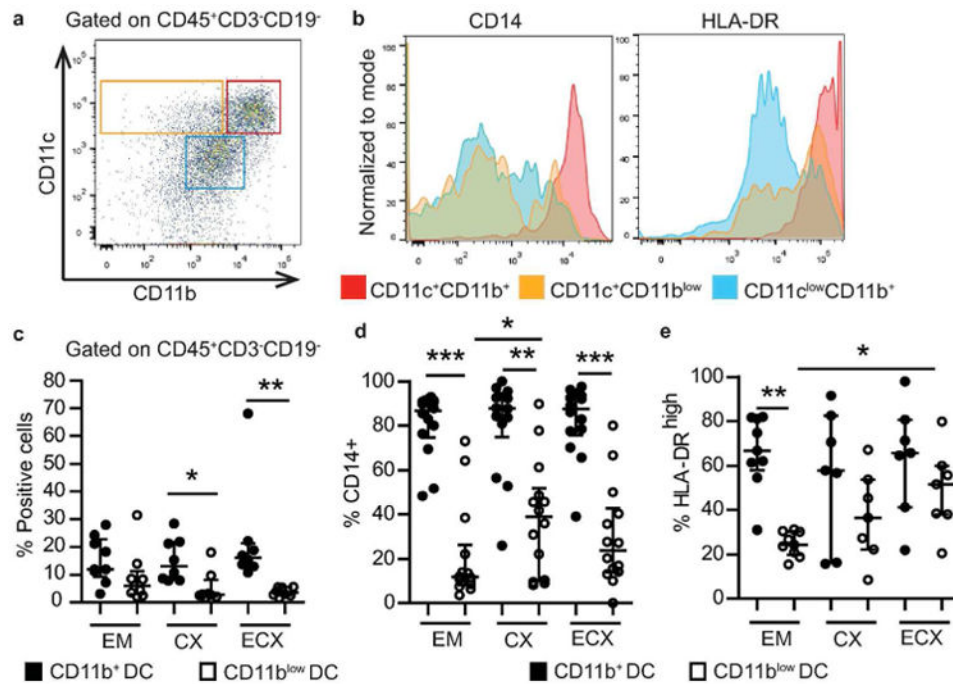
Figure 1. Characterization of CD11c$^+$ DCs in FRT tissues
(a) Representative dot plot showing three distinct populations based on CD11c and CD11b expression, after gating on CD45$^+$ immune cells and excluding CD3$^+$ T cells and CD19$^+$ B cells. **(b)** Representative overlay comparing CD14 and HLA-DR expression on the three populations identified in (a). **(c)** Percentage of CD11c$^+$CD11b$^+$ DCs (black dots) and CD11c$^+$CD11b^{low} DCs (white dots) in endometrium (EM), endocervix (CX) and ectocervix (ECX) after gating on CD45$^+$CD3$^-$CD19$^-$ cells (n=9) **(d)** Expression of CD14 (n=14) and **(e)** HLA-DR^{high} (n=9) on CD11c$^+$CD11b$^+$ DCs (black dots) and CD11c$^+$CD11b^{low} DCs (white dots) in endometrium (EM), endocervix (CX) and ectocervix (ECX). Each dot represents a single patient; matching EM, CX and ECX were obtained from each patient. Horizontal lines represent the median ± IQR. Statistical analysis was performed using the non-parametric Kruskal-Wallis test with Dunn's post-test correction for multiple comparisons. *p<0.05; **p<0.01; ***p<0.001
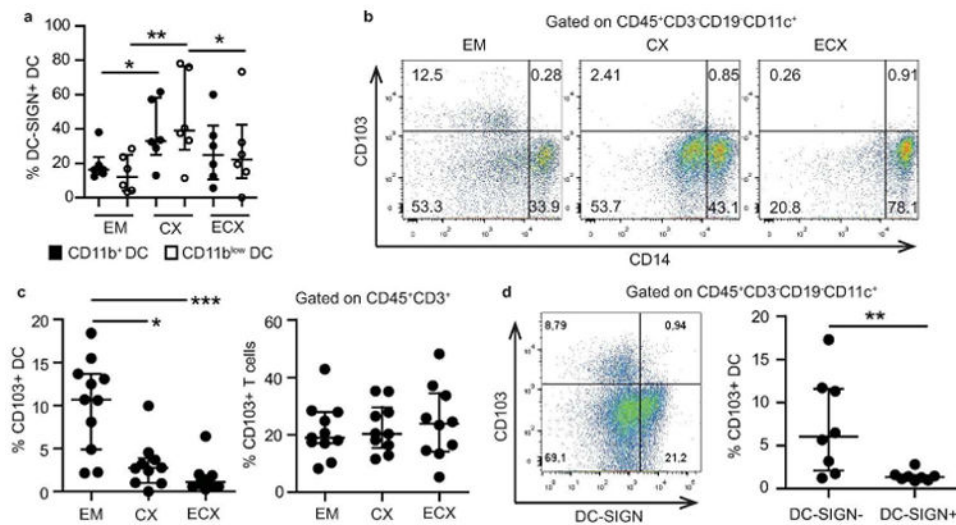
Figure 2. Expression of DC-SIGN and CD103 on DCs from the FRT

(a) Percentage of DC-SIGN+ DCs within CD11b+ DCs (black dots) and CD11b^low DCs (white dots) in endometrium (EM), endocervix (CX) and ectocervix (ECX). Horizontal lines represent the median ± IQR (n=6). (b) Representative dot plot of CD103 expression versus CD14 expression on CD11c+ cells from EM, CX and ECX. (c) Percentage of CD103+ DCs in EM, CX and ECX after gating on CD11c+CD14- cells (left graph) or on CD3+ T cells (right graph). The same patients are shown in both graphs (n=11). Each dot represents a single patient; matching EM, CX and ECX were obtained from each patient. (d) Representative dot plot and graph showing the lack of coexpression of DC-SIGN and CD103 on CD11c+ DCs from the EM. Each dot represents a single patient (n=8). Horizontal lines represent the median ± IQR. *p<0.05; **p<0.01; ***p<0.001. Statistical analysis was performed using the non-parametric Kruskal-Wallis test with Dunn's post-test correction for multiple comparisons (a and c) and the non-parametric Mann-Whitney U test (d).
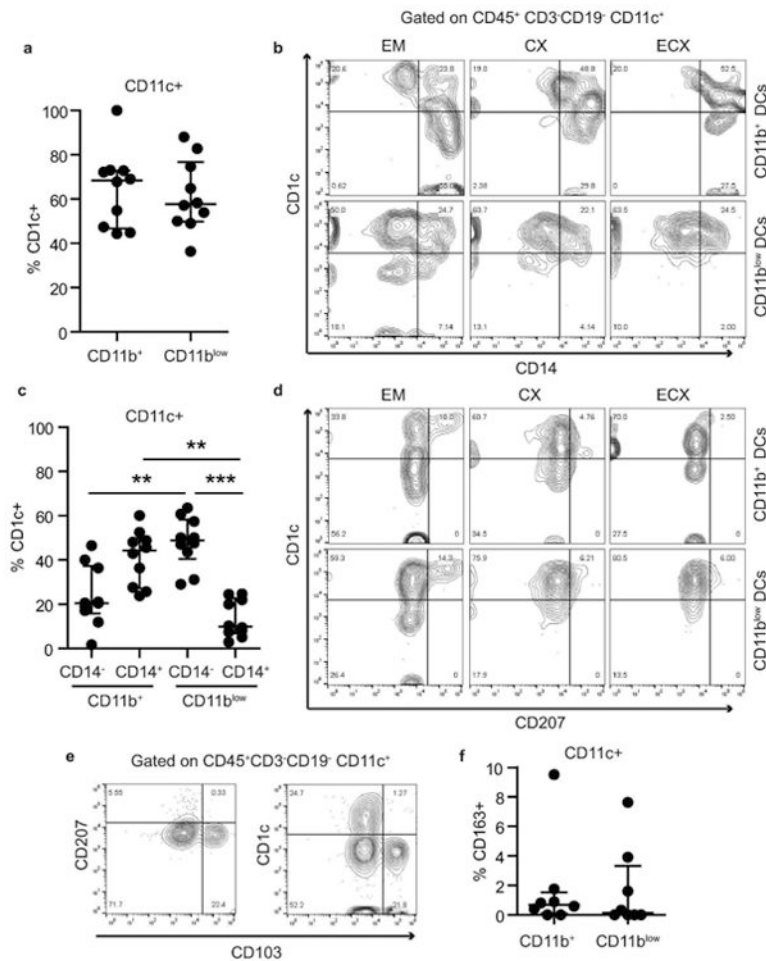
Figure 3. Identification of CD1c+ myeloid DCs in EM, CX and ECX
(a) Percentage of CD1c$^+$ DCs after gating on CD11c$^+$CD11b$^+$ and CD11c$^+$CD11b^{low} cells. (b) Representative contour plot of CD14 and CD1c expression on CD11c$^+$ cells from EM, CX and ECX. Top row shows CD11c$^+$CD11b$^+$ cells and bottom row CD11c$^+$CD11b^{low} cells. (c) Percentage of CD1c$^+$ DCs co-expressing or not CD14 after gating on CD11c$^+$CD11b$^+$ and CD11c$^+$CD11b^{low} cells. Statistical analysis was performed using the non-parametric Kruskal-Wallis test with Dunn's post-test correction for multiple comparisons (d) Representative contour plot of CD207 and CD1c expression on CD11c$^+$ cells from EM, CX and ECX. Representative of 3 independent experiments with 3 different women. (e) Representative contour plot of CD103 versus CD207 and CD1c expression on CD11c$^+$ cells from EM, CX and ECX. Representative of 3 independent experiments with 3 different women. (f) Percentage of CD163$^+$ DCs after gating on CD11c$^+$CD11b$^+$ and CD11c$^+$CD11b^{low} cells. For a, c and f, dots represent combined results for different tissues from 4 women (matching EM, CX and ECX from 3 women plus one single EM from a different woman). Horizontal lines represent the median ± IQR. **p<0.01; ***p<0.001.
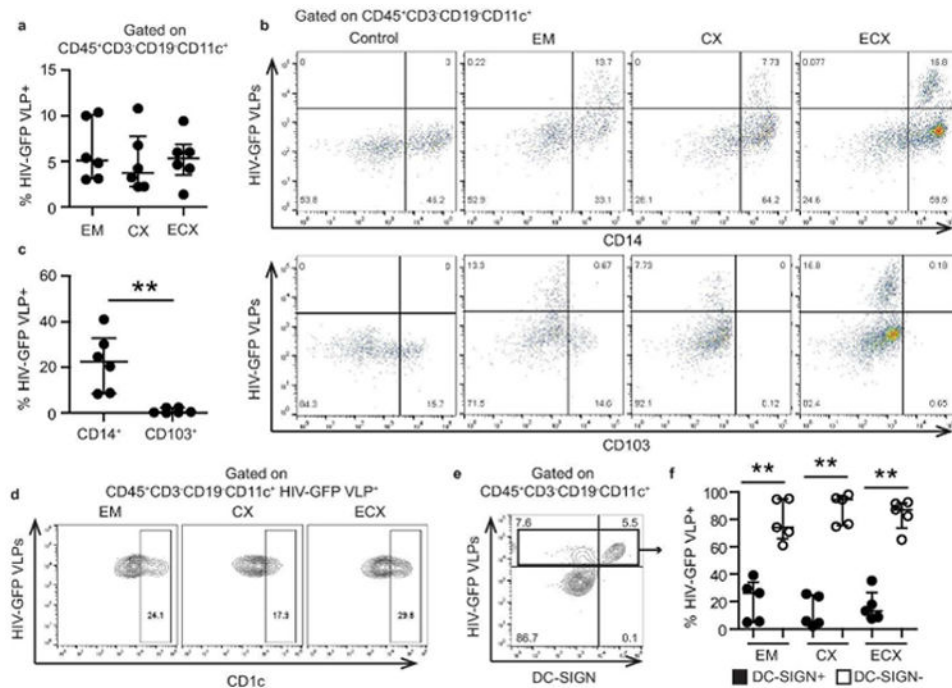
Figure 4. HIV capture by DCs from the FRT

(a) Comparison of HIV-GFP VLPs capture by CD11c$^+$CD14$^+$ cells from the EM, CX and ECX from 6 different individuals; matching EM, CX and ECX were obtained from each patient. (b) Mixed cell suspensions from endometrium (EM), endocervix (CX) and ectocervix (ECX) incubated with HIV-GFP VLPs BaL.26 env or media (control) for 1h. Dot plots show cells gated as CD45$^+$ CD3$^-$CD19$^-$ CD11c$^+$. Cells that capture the virus appear as GFP$^+$. Representative result with matched tissues from the same donor. (c) Comparison of HIV-GFP VLPs capture by CD11c$^+$CD14$^+$ cells or CD103$^+$ DCs from the EM (n=6). Each dot represents an individual patient. ** P<0.01. (d) Representative contour plot of CD1c expression on HIV-VLP+ cells from EM, CX and ECX. Representative of 3 independent experiments with 3 different women. (e) Representative contour plot of DC-SIGN and HIV-VLP capture after gating on CD11c$^+$ cells (f) Percentage of DC-SIGN+ and DC-SIGN- cells within HIV-GFP VLP$^+$ cells in EM, CX and ECX (n=5). Matching EM, CX and ECX were obtained from each patient. Horizontal lines represent the median ± IQR. Statistical analysis was performed using the non-parametric Mann-Whitney U test.
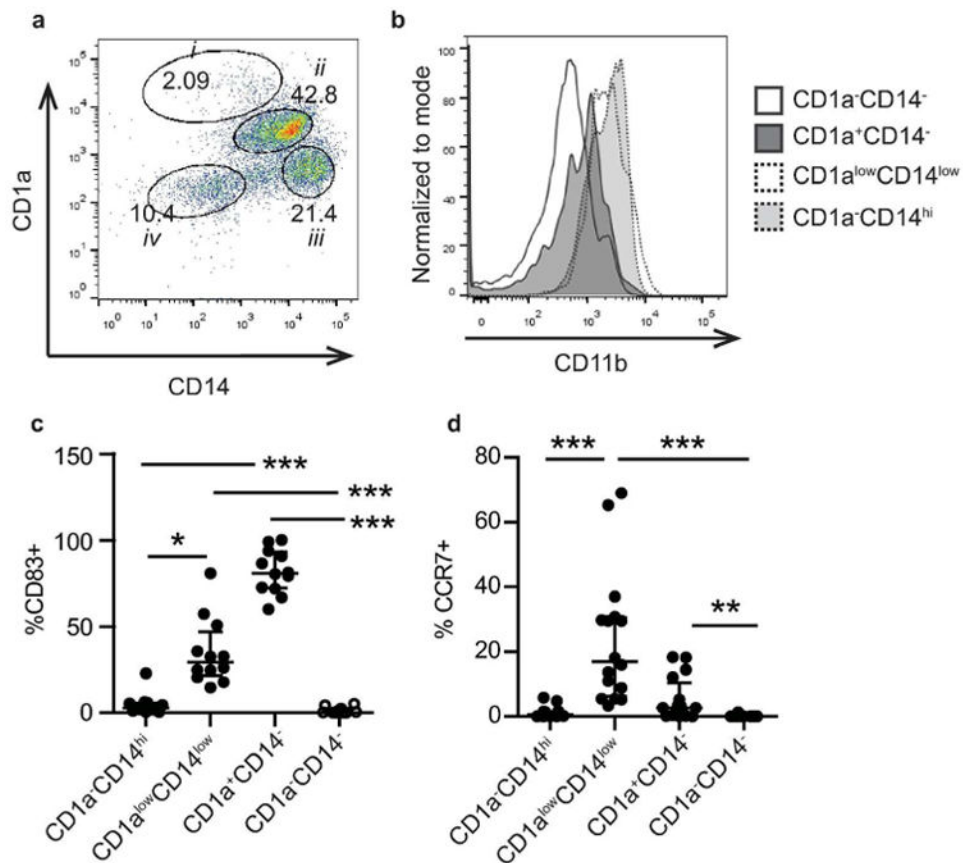
Figure 5. CD1a expression and maturation of DCs in the FRT
(a) Representative dot plot showing expression of CD1a and CD14 (gated on CD45^{+}, CD3^{-}CD19^{-}CD11c^{+}) and (b) overlay of CD11b expression in the different populations. (c) Percent of CD83^{+} and (d) CCR7^{+} DCs on CD1a^{-}CD14^{hi}, CD1a^{low}CD14^{low}, CD1a^{+}CD14^{-} and CD1a^{-}CD14[-]cells. Dots represent combined results for the different tissues from 5 women for CD83 (matching EM, CX and ECX from 4 women plus one single EM from a different woman) and from 8 women for CCR7 (matching EM, CX and ECX from 4 women and single EM from 4 women). Horizontal lines represent the median ± IQR. *p<0.05; **p<0.01; ***p<0.001. Statistical analysis was performed using the non-parametric Kruskal-Wallis test with Dunn's post-test correction for multiple comparisons.
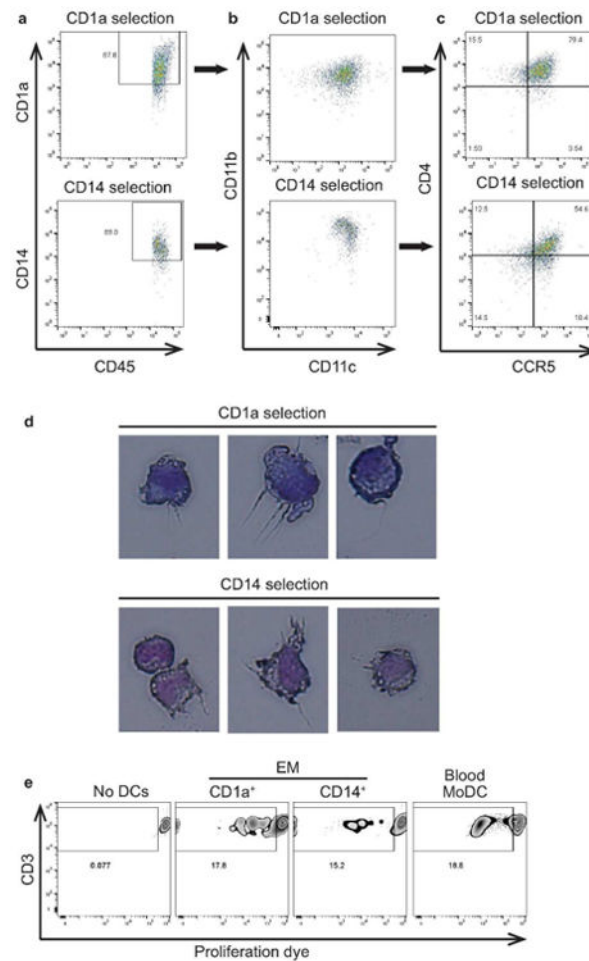
Figure 6. Characterization of CD1a+ and CD14+ bead selected cells
(a) Representative example of purity (b) CD11c and CD11b expression and (c) CD4 and CCR5 expression on EM cells after CD1a+ (top) or CD14+ (bottom) magnetic bead selection (representative of n=11). (d) Morphological characteristics of the isolated cells after Giemsa staining (representative of n=2). (e) Proliferation of blood naïve T cells after allogeneic stimulation with endometrial DCs (CD1a and CD14 selection) or with in vitro generated monocyte-derived DCs (blood MoDCs). Representative of 5 different experiments with 5 different women.
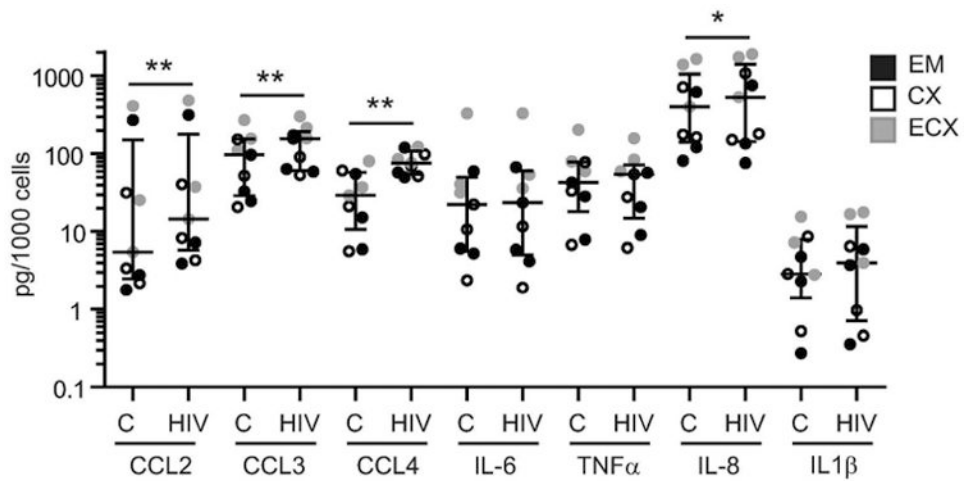
Figure 7. Secretion of cytokines and chemokines after HIV challenge of CD14^{+} cells from EM, CX and ECX

Secretion levels (pg/1000 cells) after 3h stimulation with HIV of CD14^{+} cells from EM (black dots), CX (open circles) and ECX (grey dots). Matched EM, CX and ECX were obtained from 3 different women. Statistical analysis was performed using the paired non-parametric Wilcoxon signed Rank test. Horizontal lines represent the median ± IQR. *p<0.05; **p<0.01.
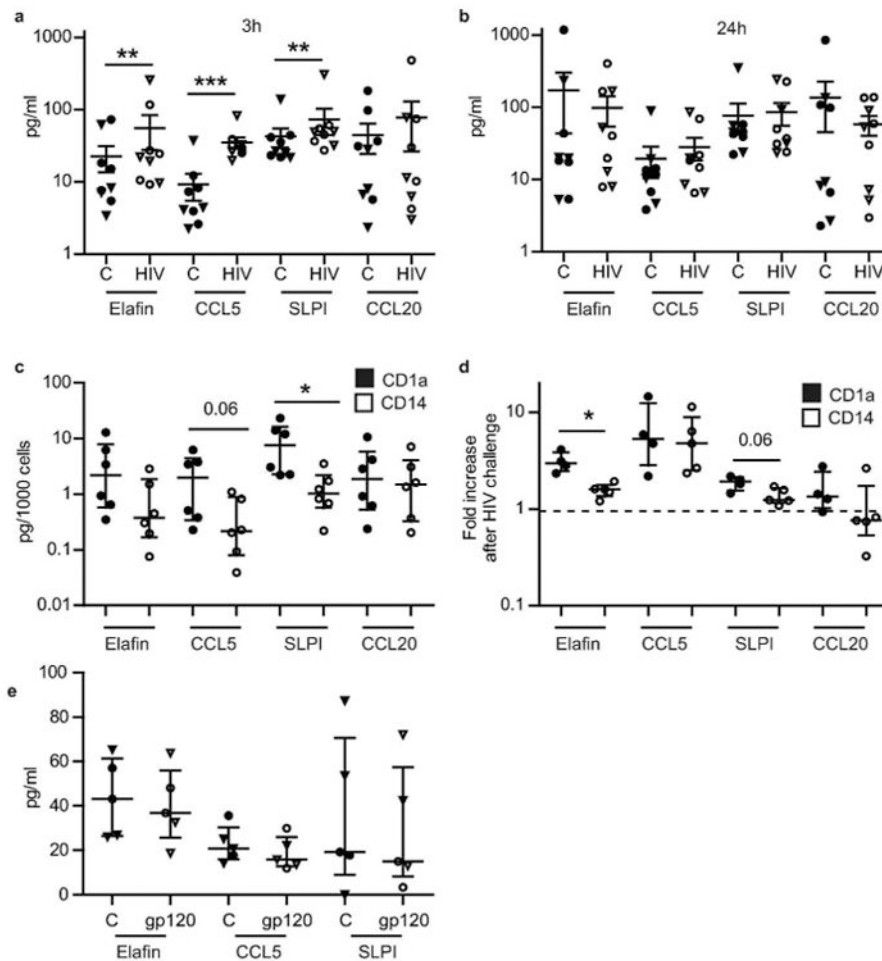
Figure 8. Secretion of antimicrobials after HIV stimulation of CD1a⁺ and CD14⁺ selected cells from the endometrium

(a) Secretion levels (pg/ml) of elafin, CCL5 (RANTES), SLPI and CCL20 in the absence of HIV stimulation (black points; C=control) or after 3h of stimulation with HIV (white points). **(b)** Secretion levels by the same cells shown in (a) 21h after removing the initial 3h supernatants. Results from cells selected using CD1a (triangles; n=4) or CD14⁺ (circles; n=5) magnetic beads are shown combined. **(c)** Baseline secretion levels at 3h adjusted by cell number (pg/1000 cells), produced by CD1a⁺ selected cells (black dots; n=6) or CD14⁺ selected cells (white dots; n=6). **(d)** Fold increase in secretion levels after HIV challenge, normalized to their own control under no HIV stimulation (control=1, dash line) for CD1a selected (black dots; n=4) and CD14 selected cells (white dots; n=5) **(e)** Lack of stimulatory effect of gp120 at 3h for the secretion of elafin, CCL5 or SLPI (n=5). Each dot represents a single patient (EM). Horizontal lines represent the median ± IQR. *p<0.05; **p<0.01; ***p<0.001. Statistical analysis was performed using the paired non-parametric Wilcoxon signed Rank test (a, b and e) and the non-parametric Mann-Whitney U test (c and d).
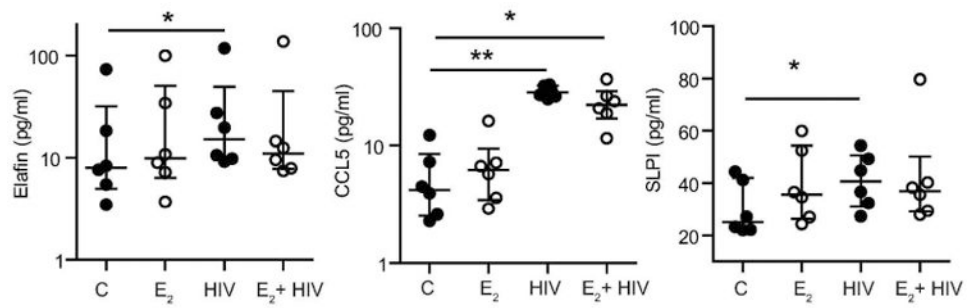
Figure 9. Effect of E$_2$ on elafin, CCL5 and SLPI secretion by DCs in response to HIV

Secretion levels of elafin, CCL5 and SLPI after pretreatment with E$_2$ prior to HIV stimulation for 3h (white dots) compared to production in the absence of E$_2$ (black dots). Results from DCs selected using CD1a or CD14$^+$ magnetic beads are shown combined. Each dot represents a single patient (EM; n=6). Horizontal lines represent the median ± IQR. *p<0.05; **p<0.01. Statistical analysis was performed using the non-parametric Friedman test with Dunn's post-test correction for multiple comparisons.

Table 1

Characteristics of the women included in the study.

	Premenopausal	Postmenopausal
Number of women	22	34
Age Median (range)	43 (27-51)	60 (45-75)
Menstrual stage		
Proliferative	72.7%	
Secretory	27.3%	
Atrophic		100%